DOI: 10.1002/adma.200600231

Isotopically Enriched ^{10}BN Nanotubes**

By *Jun Yu, Ying Chen,* Robert G. Elliman,* and *Mladen Petravic*

Protection against the hazards of space radiation (solar flares, galactic cosmic radiation) is a major challenge to human travel in deep space.[1,2] Special shielding materials, including materials consisting of mainly light elements such as hydrogen, boron, and lithium, will be required. However, additional shielding layers will add extra weight to the spaceship, which increases flight costs as more fuel is needed. In order to maintain low weight while increasing safety, reliability, and functionality, it has been proposed that the body of new spacecraft could also work as an effective shielding layer and possibly store energy, as well as be integrated with sensors.[3] This multifunctional layer requires new materials that should have different properties that meet these requirements. Carbon nanotubes (CNTs) are one of the future materials under consideration because of their light weight, excellent mechanical properties, and possible energy-storage ability.[4] We propose here that isotopically enriched ^{10}BN nanotubes, which have similar properties to CNTs, could be a better material owing to their better radiation-shielding properties and stronger resistance to oxidation. We demonstrate the synthesis of ^{10}BN nanotubes for the first time with a high yield and in large quantities using a ball-milling/annealing process. The special role of high-energy ball-milling in reducing the nitriding temperature, leading to the growth of thin, cylindrical tubes, is revealed.

BN nanotubes (BNNTs) have the same nanotubular structure as CNTs and can be regarded as a seamless cylinder rolled up from a sheet of the BN (002) basal plane. As B and N are the two neighboring elements of C in the periodic table; a similarly low density is expected for BNNTs. It has been confirmed that BNNTs also exhibit extremely high strength, similar to CNTs. A Young's modulus of 1.22±0.24 TPa was measured for multiwalled BN nanotubes,[5] which is comparable to that of CNTs (1.3–1.8 TPa).[6,7] BN nanotubes are also as stiff as CNTs.[8,9] ^{10}B is a well-known efficient neutron absorber with a very high neutron-capture cross section (over 3800 barn).[10] Therefore, ^{10}B and related compounds are widely used as the inner shielding layer inside nuclear reactors. ^{10}BN should be a better neutron absorber than normal BN because of a higher content of ^{10}B (almost 50 %). Normal BN contains mainly ^{11}B (>80 at %) and less than 20 at % of ^{10}B. In addition, diluted ^{10}B in ^{10}BN produces less secondary radiation than pure ^{10}B. Therefore, ^{10}BN is expected to exhibit a good shielding effect against space radiation. Although BN nanotubes containing the natural abundance of ^{11}B have been produced previously,[11,12] pure ^{10}BN nanotubes have not been achieved by any other methods previously. In addition, the special role of a ball-milling treatment and 2D crystalline growth of thin, cylindrical nanotubes are reported for the first time.

Scanning electron microscopy (SEM) analysis with a field-emission Hitachi S4500 microscope was used to examine the morphology of nanotube samples. The SEM image in Figure 1 shows a high yield of nanotubes, some BN layers, and a few Fe catalyst particles, which were obtained from the enriched ^{10}B powders first ball-milled for 150 h, followed by annealing at 1100 °C for 6 h in NH_3 gas. Transmission electron microscopy (TEM) analysis using a Philips CM300 microscope revealed a well-crystallized, parallel-walled tubular structure (Fig. 1 inset) and no other tubular structures (i.e. bamboo- or conelike structures) were found. ^{10}BN nanotubes with different diameters (up to 100 nm) and lengths (up to 100 μm) can also be produced by varying the growth conditions and atmosphere. For example, nanotubes with a larger diameter (>50 nm) can be produced by annealing at a higher temperature of 1200 °C for a longer period of time.

X-ray energy dispersive analysis (EDS) confirmed that the nanotube consists of elemental B and N, as indicated clearly by the pronounced B and N peaks of the spectra in Figure 2a.

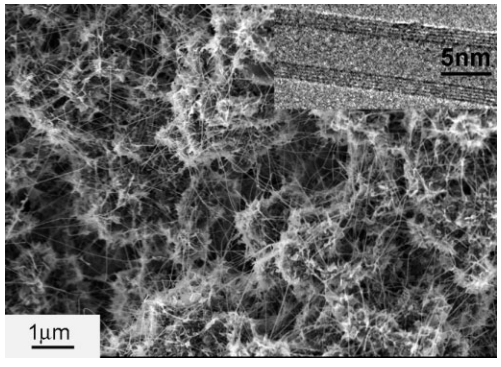

Figure 1. SEM image of ^{10}BN nanotubes produced by annealing of the milled ^{10}B powder at 1100 °C for 6 h in NH_3. The inset shows a typical transmission electron microscopy (TEM) image showing parallel fringes, indicating a well-crystallized, multiwalled, cylindrical structure.

[*] Prof. Y. Chen, J. Yu, Prof. R. G. Elliman, Dr. M. Petravic
Department of Electronic Materials Engineering
Research School of Physical Sciences and Engineering
The Australian National University, Canberra, ACT 0200 (Australia)
E-mail: ying.chen@anu.edu.au

[**] The authors gratefully thank Dr. John Fitz Gerald and the staff at the Electron Microscopy Unit for their help in assisting microscopy analyses. We also acknowledge Dr. Steve Harris and Dr. Robert C. Singleterry, Jr. for stimulating discussions. This work is, in part, supported by the Australian Research Council under a Discovery Research grant.

ADVANCED MATERIALS

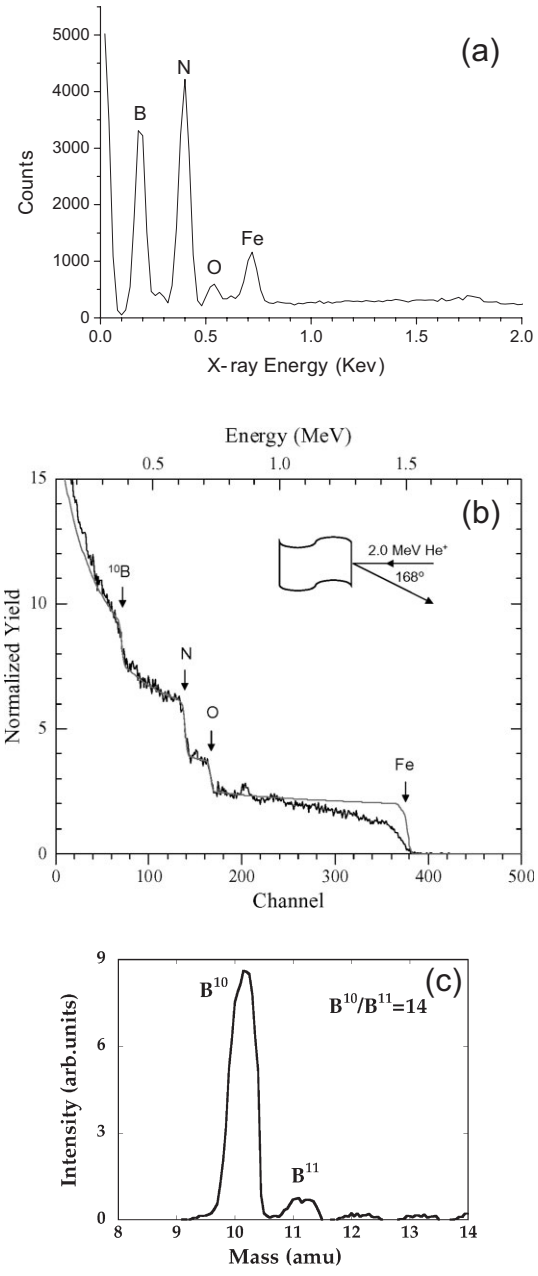

Figure 2. a) EDS spectra of ^{10}BN nanotubes showing the presence of B and N and low levels of O and Fe; b) Rutherford backscattering spectra taken from a ^{10}BN nanotube pellet using a 2.0 MeV He beam; c) Secondary ion mass spectrometry of the same ^{10}BN nanotube sample, showing the dominant presence of ^{10}B over ^{11}B.

Low levels of oxygen are probably due to exposure to air. Both Rutherford backscattering spectrometry (RBS) and secondary ion mass spectrometry (SIMS) were employed to examine the content of ^{10}B in the nanotube samples. Figure 2b reveals the presence of ^{10}B, as well as O, N, and Fe, in good agreement with EDS results. The SIMS spectrum in Figure 2c confirms the dominant presence of ^{10}B over ^{11}B. The intensity ratio of ^{10}B to ^{11}B peaks is about 14:1, which is consistent with the ^{10}B content (96 at %) of the starting material. These results clearly demonstrate a successful synthesis of ^{10}BN nanotubes.

The control over the nitriding reaction between ^{10}B and NH_3 gas is crucial for the formation of thin, cylindrical ^{10}BN nanotubes that contain fewer defects and exhibit stronger mechanical properties than other nanostructures.[4] To avoid the formation of large crystals or thick, bamboo-type nanostructures through fast 3D crystalline growth, nitriding reactions at lower temperatures with the formation of unique (002) basal planes over catalyst particles are required. This can be achieved by ball-milling the starting ^{10}B powders. The nitriding reactions of ^{10}B samples with and without milling treatment were investigated using thermogravimetric analysis (TGA) with a Shimazu TGA-50 instrument. ^{10}B samples were heated up to 1200 °C at a heating rate of 20 °C min^{-1} in a nitrogen gas flow of 50 ml min^{-1}. The TGA curves of samples milled for different times are compared in Figure 3a. The sample weight increases as the temperature increases owing to the formation of BN as the end product of the nitriding reaction ($2B + N_2 \rightarrow 2BN$). The differences in weight gain correspond to different degrees of nitridation. The starting ^{10}B sample without milling treatment has only a 4.45 % weight

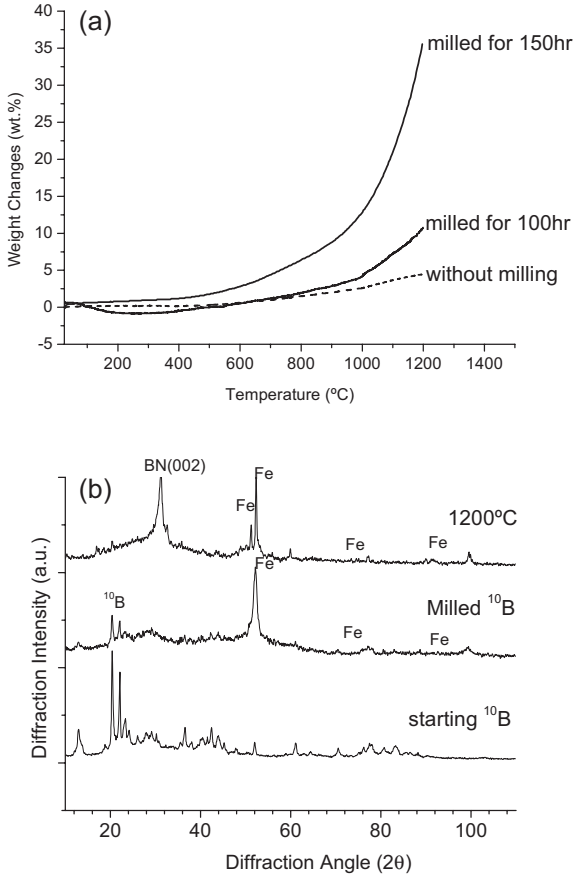

Figure 3. a) TGA curves of the sample weight changes as a function of temperature for ^{10}B samples without milling treatment and after milling for different times; b) XRD patterns taken from the starting crystalline ^{10}B sample, after ball-milling for 150 hours, and the milled ^{10}B after heating to 1200 °C with a TGA analyzer.

increase, while the 100 and 150 h milled samples have weight increases of 10.1 % and 34.3 %, respectively. These results show that longer milling times lead to higher degrees of nitridation. The TGA curves also indicate that high-energy ball-milling reduces the onset temperature of the nitriding reaction from about 1000 to 600 °C, so that a full nitridation can be achieved at a temperature below 1200 °C. X-ray powder diffraction (XRD) analysis confirmed the formation of the BN phase (Fig. 3b).

The faster nitriding reaction and lower reaction temperature are a consequence of the new structure of the milled material and the presence of the metal catalyst particles introduced by the ball-milling treatment. During high-energy ball-milling, powder particles are repeatedly flattened, fractured, and welded. Every time two steel balls collide or one ball contacts the chamber wall, particles are trapped between the surfaces.[13,14] Such high-energy impacts severely deform the particles/planes and create atomically fresh surfaces, as well as a high density of dislocations and other structural defects. Such structural changes can be seen clearly from the XRD patterns shown in Figure 3b. The starting ^{10}B has a well-crystallized hexagonal structure, while a highly disordered structure was produced after ball-milling for 150 h at room temperature, as indicated by the correspondingly broadened diffraction peaks. The high defect density induced by ball-milling can accelerate the diffusion process during reactions.[15] Alternatively, the deformation and fracturing of particles causes continuous size reduction and can lead to a reduction in diffusion distances. This can also reduce the reaction temperatures significantly.[16] Fe diffraction peaks in Figure 3b indicate that iron was incorporated in the ^{10}B sample during milling from the steel balls and the milling container as contamination.[11e,12] The average metal content determined by EDS is 1.6 at % Fe and 0.31 at % Cr, which can be controlled by varying the milling intensity and times. The Cr peak cannot be seen in the enlarged spectra in Figure 2a, which shows pronounced B and N peaks in a low-energy range. These Fe and Cr particles actually act as a catalyst, enhancing nanotube formation during the subsequent annealing.[12] Therefore, high-energy ball-milling creates a new disordered structure mixed with metal catalysts for subsequent nitriding reactions and nanotube growth. The new structure of the milled ^{10}B is chemically more reactive than the starting ^{10}B without milling treatment and thus responsible for a faster nitriding reaction, even at lower temperatures, as detected by TGA analysis.

The lower nitriding temperature is a crucial condition for the formation of nanotubular structures. The formation of BN nanotubes, especially thin nanotubes, requires the dominance of 2D growth of the BN (002) basal planes, which only occurs at temperatures in the range from 800 to 1200 °C. At higher temperatures (above 1200 °C), bulk and 3D BN crystals are dominant. The growth of BN nanotubes was investigated at different temperatures using XRD and TEM. The XRD patterns taken from the same milled sample after annealing for 4 h at different temperatures are shown in Figure 4. The thickness of the (002) planar structures was estimated from

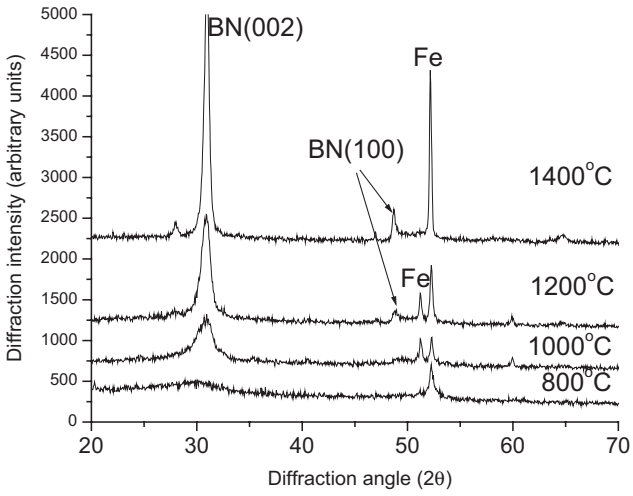

Figure 4. XRD patterns of 150 h milled ^{10}B samples after annealing at different temperatures for the same period of time (4 h) in N_2 gas.

the width of the (002) diffraction peak at half height, using the Scherrer formula.[17] The results obtained are presented in Table 1 and compared with TEM observations. For the sample annealed at 800 °C, a very broad and weak (002) peak might exist, and the calculated thickness of the material is about 5.3 nm. TEM observations revealed few (002)-oriented layers and no nanotubes, in agreement with XRD results. The annealing temperature appears to be too low, as suggested by

Table 1. Nanotube formation versus crystal growth. *D*: nanotube diameter.

Growth Temperature [°C]	Thickness of BN (002) planes [nm]	Structures observed by TEM
800	5.3	No nanotubes, few (002) layers
1000	13.7	Thin nanotubes ($D < 20$nm) Many thin (002) layers, No BN particles
1200	19.1	Thin and thick nanotubes (20 nm < D < 150 nm)
1400	47.9	No nanotubes BN particles

the TGA analysis (Fig. 3b). For the sample annealed at 1000 °C, a clear and broad (002) diffraction peak can be seen. The thickness of the (002) oriented layer is about 13.7 nm. Only thin nanotubes with a diameter (D) less than 20 nm are found in the sample, as well as some (002)-oriented material on the surfaces of B particles. When the temperature is increased to 1200 °C, the (002) peak in the XRD pattern becomes sharper and the average thickness of the (002)-oriented material increases to 19.0 nm. The appearance of a second, strong BN (100) diffraction peak in the XRD pattern (Fig. 4) suggests the start of the formation of 3D crystalline BN structures. Indeed, TEM images show some thick BN nanotubes (20 nm < D < 150 nm) and few BN crystals. After heating at

ADVANCED MATERIALS

1400 °C, XRD detects an almost perfect BN hexagonal structure with an estimated thickness (or grain size) of 47.9 nm, which is confirmed by TEM observations. No nanotubes were found under these conditions. Therefore, a low-temperature nitriding reaction with 2D crystalline growth is important for BN nanotube formation during the milling–annealing process.

^{10}BN nanotubes exhibit a strong resistance against oxidation at high temperatures. TGA analysis in an oxygen atmosphere revealed that ^{10}BN nanotubes were stable up to 900 °C under a pure oxygen gas flow (50 ml min^{-1}). A rapid weight increase, caused by the oxidation of BN nanotubes with the formation of solid boron oxides, occurred around 900 °C (heating rate of 20 °C min^{-1}), whereas multiwalled CNTs are completely oxidized below 700 °C under the same analysis conditions, consistent with previous observations.[18] Based on XRD and TEM results, this stronger resistance to oxidation could be explained by the fact that: 1) B–N bonds are more stable against oxidation; 2) newly formed B_2O_3 layers cover the nanotube surface and thus prevent further oxidation; 3) the ^{10}BN nanotubes have a well-crystallized structure with fewer structural defects.[19]

In summary, ^{10}BN nanotubes have been successfully produced using a ball-milling/annealing process. The ^{10}BN nanotubes have a well-crystallized multiwalled structure and exhibit a strong resistance to oxidation. The role of the high-energy ball-milling is to reduce the reaction temperature by creating a chemically reactive structure and to introduce metal catalysts into ^{10}B. A low-temperature nitriding reaction with 2D crystalline growth of (002) basal planes is important for nanotube formation. ^{10}BN nanotubes are lightweight, with a density of 1.85 g cm^{-3} determined from pressed pellets, and have an excellent resistance to oxidation. They are also expected to exhibit a high neutron-absorption cross section because of the high content of ^{10}B. The successful production of high yield ^{10}BN nanotubes using a ball-milling/annealing process makes ^{10}BN nanotube samples available in large quantities for space-radiation tests.

Experimental

The ^{10}BN nanotubes were synthesized using a high-energy ball-milling/annealing process in which ^{10}B powders (enriched ^{10}B from EaglePicher containing >96 at % ^{10}B) were first milled at room temperature for 150 h in an atmosphere of ammonia (300 kPa). The treatment was conducted with a high-energy rotating ball-mill at room temperature.[11e,11f,12] A laboratory-sized stainless-steel milling container was loaded with several grams of ^{10}B powders and four hardened steel balls. Ammonia gas at a starting pressure of 300 kPa was introduced into the sealed container prior to milling. The milled ^{10}B powder was then annealed in a tube furnace at 1100 °C for 6 h under a flow of ammonia gas (about 100 ml min^{-1}). For both RBS and SIMS analyses, BN nanotubes were pressed into 2 mm thick pellets at room temperature. RBS spectra were recorded using 2.0 MeV He ions at a scattering angle of 168°.

Received: February 4, 2006
Final version: April 14, 2006
Published online: July 25, 2006

[1] J. W. Wilson, *Health Phys.* **2001**, *79*, 470.
[2] J. Miller, C. Zeitlin, F. A. Cucinotta, L. Heilbronn, D. Stephens, J. W. Wilson, *Radiat. Res.* **2003**, *159*, 381.
[3] R. C. Singleterry, Jr., S. A. Thibeault, *NASA Technical Publication 210 281*, **2000**.
[4] P. M. Ajayan, O. Z. Zhou, in *Carbon Nanotubes: Synthesis, Structure, Properties, and Applications* (Eds: M. S. Dresselhaus, G. Dresselhaus, P. Avouris), Springer, Berlin **2000**, Ch. 13.
[5] N. G. Chopra, A. Zettl, *Solid State Commun.* **1998**, *105*, 297.
[6] M. M. J. Treasy, T. W. Ebbesen, J. M. Gibson, *Nature* **1996**, *381*, 678.
[7] E. W. Wong, P. E. Sheehan, C. M. Lieber, *Science* **1997**, *277*, 1971.
[8] D. Srivastava, M. Menon, K. Cho, *Phys. Rev. B: Condens. Matter Mater. Phys.* **2001**, *63*, 195 413.
[9] T. Dumitrica, *Phys. Rev. B: Condens. Matter Mater. Phys.* **2003**, *68*, 085 412.
[10] Technical Document No. EP-SSGC-HBO3, EaglePicher Technologies LLC, Quapaw, OK **2002**.
[11] a) N. G. Chopra, R. J. Luyken, K. Cherrey, V. H. Crespi, M. L. Cohen, S. G. Louie, A. Zettl, *Science* **1995**, *269*, 966. b) A. Loiseau, F. Williame, N. Demoncy, G. Hug, H. Pascard, *Phys. Rev. Lett.* **1996**, *76*, 4737. c) M. Terrones, W. K. Hsu, H. Terrones, J. P. Zhang, S. Ramos, J. P. Hare, R. Castillo, K. Prassides, A. K. Cheetham, H. K. Kroto, D. R. M. Walton, *Chem. Phys. Lett.* **1996**, *259*, 568. d) D. Golberg, Y. Bando, M. Eremets, K. Takemura, K. Kurashima, H. Yusa, *Appl. Phys. Lett.* **1996**, *69*, 2045. e) Y. Chen, J. Fitzgerald, J. S. Williams, S. Bulcock, *Chem. Phys. Lett.* **1999**, *299*, 260. f) Y. Chen, L. T. Chadderton, J. Fitzgerald, J. S. Williams, *Appl. Phys. Lett.* **1999**, *74*, 2960.
[12] Y. Chen, M. Conway, J. S. Williams, J. Zou, *J. Mater. Res.* **2002**, *17*, 1896.
[13] J. S. Benjamin, T. E. Volin, *Metall. Trans.* **1974**, *5*, 1929.
[14] D. Galy, L. Chaffron, G. Martin, *J. Mater. Res.* **1997**, *12*, 688.
[15] A. K. Bhattacharya, E. Arzt, *Scr. Metall. Mater.* **1993**, *28*, 395.
[16] Y. Chen, T. Hwang, M. Marsh, J. S. Williams, *Metall. Trans. A* **1997**, *28*, 1115.
[17] A. Guinier, *Theorie et technique de la Radio-Crystallographie*, Dundod, Paris **1956**.
[18] W. Han, W. Mickelson, J. Cumings, A. Zettl, *Appl. Phys. Lett.* **2002**, *81*, 1110.
[19] Y. Chen, J. Zou, S. J. Campbell, G. Le Caer, *Appl. Phys. Lett.* **2004**, *84*, 2430.

